Measurement Report: Polycyclic aromatic hydrocarbons (PAHs) and their alkylated (RPAHs), nitrated (NPAHs) and oxygenated (OPAHs) derivatives in the global marine atmosphere: occurrence, spatial variations, and source apportionment

Rui Li[a, b, *, 1], Xing Liu[c, 1], Yubing Shen[a], Yumeng Shao[a], Yining Gao[a], Ziwei Yao[c], Xi Liu[d], Guitao Shi[a,*]

a Key Laboratory of Geographic Information Science of the Ministry of Education, School of Geographic Sciences, East China Normal University, Shanghai, 200241, PR China

b Institute of Eco-Chongming (IEC), 20 Cuiniao Road, Chenjia Town, Chongming District, Shanghai, 202162, China

c State Environmental Protection Key Laboratory of Coastal Ecosystem, National Marine Environmental Monitoring Center, Dalian 116023, China

d Agilent Technologies (China) Ltd., Inc., Beijing, 100102, China

* Corresponding author

Prof. Li (rli@geo.ecnu.edu.cn) and Prof. Shi (gtshi@geo.ecnu.edu.cn)

[1]Rui Li and Xing Liu contributed to the work equally.

Abstract

Ambient polycyclic aromatic hydrocarbons (PAHs) and their derivatives have severe adverse impacts on organism health and ecosystem safety. However, their global distributions, sources, and fate in marine aerosol remain poorly understood. To fill the knowledge gap, high-volume air samples were collected along a transect from China to Antarctica and analyzed for particulate PAHs and derivatives. The highest PAH concentrations in marine aerosols were observed in the Western Pacific (WP: 447 ± 228 pg/m³), followed by the East China Sea (ECS: 195 pg/m³), Antarctica Ocean (AO: 111 ± 91 pg/m³), East Australian Sea (EAS: 104 ± 88 pg/m³), and the lowest in the Bismarck Sea (BS: 17 ± 12 pg/m³). Unexpectedly, PAH concentrations in the AO were even higher than those in the EAS and BS. This could be attributed to the relatively low anthropogenic PAH emissions from Australia and Papua New Guinea, whereas AO is often affected by emissions from engine combustion and biomass burning. In contrast to the distribution of PAHs, OPAH levels in the EAS were much higher than those in the AO. It was assumed that OPAHs mainly originated from the

secondary formation of parent PAHs through reactions with O_3 and OH radicals, both of which are more prevalent in EAS. Several source apportionment models suggested that PAHs and their derivatives in marine aerosol are dominated by three sources: coal burning and engine combustion emissions (56%), wood and biomass burning (30%), and secondary formation (14%). Specifically, marine aerosols in ECS and WP were significantly affected by coal burning and engine combustion, while those in BS and EAS were mainly influenced by wildfire and coal combustion. AO was primarily dominated by biomass burning and local shipping emissions.

1. Introduction

Polycyclic aromatic hydrocarbons (PAHs), a class of semi-volatile organic compounds (SVOCs), are often considered carcinogenic and mutagenic pollutants (Li et al., 2023; Wei et al., 2021). These pollutants are generally released from the combustion of fossil fuels, biofuels, oil spills, and other biogenic sources (Li et al., 2021a; Zhang et al., 2023). Due to long-range atmospheric transport (LRAT), PAHs emitted from industrial and residential sources can often be transported to remote regions such as the open ocean and polar areas (Li et al., 2021a; Zhang et al., 2023). These PAHs species can exert toxic effects on marine organisms through dry and wet deposition (Li et al., 2021b). Additionally, high levels of oxidants (OH radicals, NO_3 radicals, and O_3) enriched in the atmosphere can promote the transformation of parent PAHs into their derivatives (RPAHs, NPAHs, and OPAHs) (Zimmermann et al., 2013). Compared to parent PAHs, nearly all of these derivatives exhibit higher toxic potency to aquatic animals due to their direct-acting mutagenicity (Bandowe and Meusel, 2017; Kovacic and Somanathan, 2014). Therefore, it is crucial to investigate the spatial characteristics of PAHs and their derivatives and to identify the key factors and potential sources of atmospheric PAHs. This knowledge is essential for reducing potential damage to ocean ecosystems and improving marine environmental management.

A growing body of literature have explored the spatial variations of ambient PAHs in the marine atmosphere. For instance, Kang et al. (2017) found that atmospheric PAH concentrations in the East China Sea ranged from 0.16 to 17.6 ng/m³ (average: 3.87 ng/m³), with these compounds being dominated by 4-ring PAHs. Subsequently, Neroda et al. (2020) investigated PAHs in the aerosols of the North-West Pacific Ocean, estimating total PAH levels ranging from 17.1 pg/m³ (northern part of the Sea of Japan) to 142 pg/m³ (La Perouse Strait). More recently, Wietzoreck et al. (2022)

59 reported that the mean concentrations of total PAHs, RPAHs, OPAHs, and NPAHs in the gas and

60 particulate phases in the Mediterranean were 2.99 ± 3.35 ng/m³, 0.83 ± 0.87 ng/m³,

61 0.24 ± 0.25 ng/m³, and 4.34 ± 7.37 pg/m³, respectively. Most current studies about PAHs in marine

62 aerosols focus on regional scales, particularly in oceans with intense anthropogenic activities, while

63 few studies reveal the spatial distributions of PAHs and their derivatives in remote oceans (e.g., the

64 polar oceans) or on a global scale. The Southern Ocean is often considered a remote and pristine

65 sea, and its local ecosystem is more sensitive to PAHs and their derivatives. However, to date, only

66 a few studies have investigated the spatial variations of ambient PAHs in the marine aerosol within

67 this region. Cabrerizo et al. (2014) first demonstrated that the volatilization from soil and snow

68 might be the major sources of ambient PAHs in the Southern Ocean and Antarctica. Very recently,

69 Overmeiren et al. (2024) analyzed the components of PAHs and OPAHs at a coastal site in

70 Antarctica and found that phenanthrene, pyrene, and fluoranthene derived from volcanic emissions

71 accounted for the major fractions of PAHs. To the best of our knowledge, only Zhang et al. (2022)

72 investigated the global variations of PAH components in marine aerosols and found a clear

73 latitudinal gradient from the Western Pacific to the Southern Ocean. They also identified coal

74 combustion as the major contributor to ambient PAHs (52%). Zetterdahl et al. (2016) also revealed

75 that the shipping emission might play an important role on the PAHs in the marine atmosphere.

76 They verified the new regulation (since late 2014) about the use of low-sulfur residual marine fuel

77 oil instead of heavy oil significantly altered the chemical compositions of PAHs (increasing the low-

78 ring components, while decreasing the high-ring components). Unfortunately, nearly all current

79 studies focus solely on PAHs and OPAHs in regional oceans, whereas no study has comprehensively

80 investigated the spatial variations of particulate PAHs and all their derivatives on a global scale.

81 Moreover, the source contributions of PAH derivatives in different oceans remain unknown. It is

82 important to fill the knowledge gaps regarding the compositions, sources, and fate of PAH

83 derivatives in the marine atmosphere on a global scale.

84 In our study, an expedition research cruise aboard a Chinese research vessel from October 2019

85 to April 2020, traveling from China to Antarctica, provided a unique opportunity to reveal the

86 distributions, compositions, and fate of parent PAHs and their derivatives (RPAHs, NPAHs, and

87 OPAHs). Taking advantage of this unique opportunity, our study aims to: (1) investigate the

latitudinal gradient of PAHs and their derivatives; (2) study the major factors contributing to the spatial variations; and (3) identify the sources using a Positive Matrix Factorization (PMF) model.

2. Material and methods

2.1 The shipping cruise and sample collection

The expedition research cruise of Chinese research vessel took place from October 22 in 2019 to April 21 in 2020. The expedition sailed from Shanghai in China, crossing Pacific, Indian Ocean, and Southern Ocean and finally arrived at Antarctica. Then, the return route was also from Antarctica to Shanghai, in China. The detailed information of the shipping route is depicted in Figure S1 and 1.

Atmospheric samples were collected using a high-volume air sampler (HVAS, TISCH Environmental, USA), positioned on the upper deck of the RV/Xuelong, approximately 30 m above sea level. Aerosol particles were captured on Whatman quartz fiber filters (QM-A, 20.3 cm × 25.4 cm, pore size 2.5 μm), which were pre-baked at around 500 °C for over 4 hours to eliminate water and organic residues. The HVAS operated at an airflow rate of approximately 1.2 m³ min⁻¹, with each sampling event lasting 2 to 3 days, resulting in total air volumes typically ranging from 3000 to 4000 m³. During this time, atmospheric particles were collected along the cruise path, spanning approximately 2 to 4 degrees of latitude, yielding a single aggregate sample per filter. To minimize potential contamination from the research vessel, a wind direction sensor directed the HVAS, ensuring that only air masses from a sector of approximately 120° on either side of the vessel's central trajectory were sampled. After collection, individual filters were carefully separated, folded, wrapped in aluminum foil, placed in zip-lock bags, and stored in the dark at -20 °C until particle characterization analyses began. A total of 35 samples were collected during the cruise, along with 2 field blank samples prepared from filters mounted in the HVAS with an air pump flow rate set to 0. The sampling protocols for the blanks mirrored those described above regarding duration, filter mounting, collection, transport, observation, and measurements.

2.2 Chemical analysis

Automated Soxhlet extraction with DCM (JT Baker, Avantor group, Poland), pesticide residue grade) in a B-811 extraction unit (Büchi, Flawil, Switzerland) for PAH, NPAH, and OPAH analysis was employed. The extract was cleaned up using a silica column (with 1 cm i.d. as open tube using

117   5 g of silica (Merck, Darmstadt, Germany), 0.063-0.200 mm, activated at 150 °C for 12 h, 10%

118   deactivated with water) and 1 g Na_2SO_4 (Merck, Darmstadt, Germany). For the analysis of RPAHs,

119    $PM_{2.5}$ samples were extracted based on the procedure described in Iakovides et al. (2021). A gas

120   chromatograph (Agilent 7890B GC) coupled with the mass spectrometer (Agilent 5977B MS) was

121   employed to determine the concentrations of PAH, NPAH, and OPAH species. The detailed analysis

122   method and quality control of these PAHs and their derivatives are introduced in the supporting

123   information (Text S1 and Table S1). The reference standards of PAHs (Pyr-d10 and BaP-d12; Wako

124   Pure Chemicals, Osaka, Japan), OPAHs (purchased from First Standard (Sigma, America), RPAHs

125   (AccuStandard (New Haven, CT, USA)), and NPAHs (2-fluoro-7-nitrofluorene; Aldrich Chemical

126   Company, Osaka, Japan) were used for calibrating quantification.

127   2.3 Source apportionment

128   As a typical receptor-based model used for source apportionment, the PMF 5.0 version have

129   been widely applied to determine the potential origins of PAH and their derivatives, and to determine

130   the contribution ratios of multiple sources to these components (Sharma et al., 2016). The aim of

131   PMF model is to solve the issues of chemical mass balance between the observed concentration of

132   each PAH species and their source contributions via decomposing the input matrix into factor

133   contributions and factor profiles. The detailed equation is shown in Eq. (1). Additionally, the

134   contribution of each source for an individual component should be ensured to be non-negative.

135   Briefly, the basic principle of PMF is to determine the least object function Q when the g_{ik} must be

136   a non-negative matrix based on Eq. (2) (Jaeckels et al., 2007; Taghvaee et al., 2018).

137
$$x_{ij} = \sum_{k=1}^{p} g_{il}f_{lj} + e_{ij} \quad (1)$$

138
$$Q = \sum_{i=1}^{n}\sum_{j=1}^{m}[\frac{x_{ij} - \sum_{k=1}^{p} g_{il}f_{lj}}{u_{ij}}]^2 \quad (2)$$

139   where x_{ij} and e_{ij} represent the PAH concentrations and uncertainty of the jth component, respectively.

140   g_{il} denotes the contribution ratio of the lth source to the ith sample, f_{lj} is the ratio of the jth component

141   in the lth source, and e_{ij} denotes the residual of the jth element in the ith sample. The 2-6 factor

142   solutions were examined, and a three-factor solution was decided with the ratio of Q (robust) and Q

143   (true) reaching 0.93. The coefficients of determination (R^2) between the predicted and observed

144 concentrations of PAHs and their derivatives were shown in Table S2. The uncertainties linked with

145 factor profiles were assessed based on three error calculation methods including the bootstrap (BS)

146 method, displacement (DISP) analysis, and the combination method of DISP and BS (BS-DISP).

147 For the BS method, 1000 runs were conducted and the result has been considered to be robust

148 because all of the factors showed a mapping of above 90%. DISP analysis also demonstrated that

149 this solution was stable because the observed drop in the Q value was < 0.1% and no factor swap

150 occurred. For the BS-DISP analysis, the solution has been verified to be useful because the observed

151 drop in the Q value was < 0.5%. Moreover, both of the results from BS and BS-DISP did not show

152 any asymmetry or rotational ambiguity for all of the factors (Ambade et al., 2023; Gao et al., 2015;

153 Yan et al., 2017).

154 2.4 GEOS-Chem model

155 GEOS-Chem (v13.4.0) model was employed to estimate O_3 and OH radical concentrations

156 during Jan. 1-Dec. 31 in 2019. This model comprises of a complex chemistry mechanism of

157 tropospheric NO_x-VOC-O_3-aerosol (Park et al., 2004). This model was driven by MERRA2

158 meteorological parameters (Hamal et al., 2020; Koster et al., 2020; Qiu et al., 2020). A global

159 simulation was conducted at a spatial resolution of $2 \times 2.5°$ resolution (Qiu et al., 2020; Weagle et

160 al., 2018; Zhang et al., 2021a). The historical multi-sector anthropogenic emission dataset was

161 downloaded from Community Emissions Data System (Hoesly et al., 2018). Natural emissions

162 including wildfire, soil emission, and lightning emissions were also incorporated into the GEOS-

163 Chem model. Wildfire emissions derived from Global Fire Emissions Database (GFED) were used

164 for simulations (Chen et al., 2023). The lightning NO_X emission was collected from

165 http://geoschemdata.wustl.edu/ExtData/HEMCO/OFFLINE_LIGHTNING/v2020-03/MERRA2/

166 (Murray et al., 2012).

167 **3 Results and discussions**

168 3.1 The chemical compositions of PAHs and their derivatives in the atmosphere

169 The concentrations of 18 PAHs, 11 OPAHs, 9 RPAHs, and 7 NPAHs in 33 samples were

170 determined. The average concentrations of ΣPAHs, ΣOPAHs, ΣRPAHs, and ΣNPAHs were 157±98,

171 1920±1250, 12.1±9.5, and 3.0±1.6 pg/m^3, respectively. The total concentrations of PAHs and their

172 derivatives in the marine aerosols (Pacific and Antarctic Ocean (AO)) were significantly lower than

those in urban regions such as Harbin (86.9 ng/m^3) (Ma et al., 2020), Augsburg (1.3 ng/m^3) (Pietrogrande et al., 2011), and Southeastern Florida (3.0 ng/m^3) (Sevimoglu and Rogge, 2016). However, the PAHs concentration in our study was comparable to those in some remote regions. For instance, Cabrerizo et al. (2014) found that the total concentration of 18 particulate PAHs over AO ranged from 0.03 to 4.2 ng/m^3. Later on, Zhang et al. (2022) reported that the 15 PAHs in PM$_{2.5}$ across Pacific and AO ranged from 0.11 to 1.2 ng/m^3. Very recently, Van Overmeiren et al. (2024) revealed that the total concentrations of 15 PAHs in PM$_{2.5}$ in Antarctica was only 1.5 pg/m^3, which was even much lower than the result in our study. The large gaps for PAH concentrations between remote ocean (polar region) and urban regions might be associated with the intensity of anthropogenic emission (Shen et al., 2013; Zhang and Tao, 2009). Although the total concentration could provide the overall picture of PAHs in the global marine boundary layer, the specific compounds in PAHs also varied greatly.

Among all of the PAHs, the BbF showed the highest level (26.8±10.4 pg/m^3), followed by Ace (18.4±9.8 pg/m^3), Fluoran (16.3±8.4 pg/m^3), and the lowest one was Acy (0.12±0.05 pg/m^3) (Figure 2). Overall, the PAHs in the global marine aerosols were dominated by 3-5 ring components (~83%), which was in agreement with the result in Pacific and Indian Ocean observed by Zhang et al. (2022). It was reported that Fluoran, Acy, and Ace were often sourced from biomass or coke burning (Zhang et al., 2021c), while BbF was generally enriched in the production of wood and coal combustion (Li et al., 2022), indicating the marine aerosol could be influenced by the solid fuel burning.

Among all of the OPAHs, 1-Naphthaldehyd showed the highest concentration (852±406 pg/m^3), followed by 1,4-Chysenequione (787±386 pg/m^3), Ancenaphthenaquinone (133±75 pg/m^3), Anthraquinone (58±31 pg/m^3), and the lowest one was 5,12-Naphthacenequione (1.49±0.64 pg/m^3). In general, the absolute concentrations of OPAHs were comparable or slightly lower than those of PAHs especially in some high-latitude sites. Nevertheless, the OPAHs concentrations in our study were markedly higher than PAHs levels ($p < 0.01$). It was well known that OPAHs was often released from incomplete combustion or generated from photochemical reactions of O$_3$, OH, and NO$_3$ radicals with PAHs (Zhang et al., 2022). The higher concentrations of O$_3$ and OH radicals over tropical oceans might largely promote the PAH oxidation (Zhang et al., 2022). For RPAHs, 1,3-Dimethylnaphthalene (4.47±2.64 pg/m^3) and 2-Methylnaphthalene (4.38±2.42 pg/m^3) accounted for

the major fractions (73%) of RPAHs, while the concentrations of other species were relatively low. Wietzoreck et al. (2022) confirmed the chemical compositions of RPAHs in Middle East Seas displayed similar patterns with our study. The NPAHs in the marine aerosol were also dominated by 2-Nitronaphthalene (2.2 ± 1.1 pg/m^3) and 5-Nitroacenaphthene (2.0 ± 0.7 pg/m^3), while the contributions of other species were negligible.

3.2 The spatial variations of particulate PAHs derivatives and key meteorological factors

To reveal the spatial variations of atmospheric PAHs and the derivatives, all of the sampling sites were divided into five groups (regions): East China Sea (ECS), Western Pacific (WP), Bismarck Sea (BS), Eastern Australia Sea (EAS), and AO. The PAHs concentrations followed the order of WP (447 ± 228 pg/m^3) > ECS (195 pg/m^3) > AO (111 ± 91 pg/m^3) > EAS (104 ± 88 pg/m^3) > BS (17 ± 12 pg/m^3) (Figure 3). Based on Mann-Whitney test, the PAHs concentrations in WP were significantly higher than those in other oceans ($p < 0.05$). High levels of PAHs in WP are closely linked with the high coverage of continent-affected regions such as Southeast Asian and East Asian countries. AO showed the lower PAHs concentrations because the sea was far away from continental sources. In general, PAH levels in the remote marine atmosphere appear to be affected by long-range transport and air-seawater exchange, whereas local anthropogenic emission might be responsible for the ambient PAHs near the continent. For AO, the Antarctica continent lacks of anthropogenic activity, and thus it leads to the lower PAHs levels in the atmosphere of AO. It should be noted that both of EAS and BS were close to Australia, while the PAHs concentrations in these oceans were even lower than those in AO. It was assumed that Australia possesses very low anthropogenic PAH emission (< 10 μg/km^2) compared with many other continents (Shen et al., 2013). Although the total PAHs showed remarkably higher concentrations in ECS and WP, all of the congeners did not show the same spatial variations with the total PAHs level. For instance, Fluoran, Pyr, BeP, and BaP levels in AO were even higher than those in ECS, and the BbF levels in EAS were much higher than those in ECS. BbF generally originated from wood burning (Zhang et al., 2022a), and wildfire often occurred in the summer and autumn of Australia (Haque et al., 2021), which might elevate the BbF concentration in the marine aerosol along Australia. The simulated wildfire-related ambient benzene concentration via GEOS-Chem model (Figure S2) was utilized to establish the relationship with the ambient BbF level in the aerosols, and the correlation coefficient

231 reached 0.52 ($p < 0.05$). The result confirmed that local wildfire in Australia largely increased BbF

232 concentration in the marine aerosol.

233   The total OPAHs also exhibited marked spatial variations with the highest concentrations in

234 WP (3328 ± 1846 pg/m^3), followed by EAS (2675 ± 1452 pg/m^3), ECS (2506 pg/m^3), AO (1447 ± 865

235 pg/m^3), and the lowest one in BS (897 ± 544 pg/m^3). Different from the spatial distribution of parent

236 PAHs, OPAHs levels in EAS were much higher than those in AO and BS. It was widely

237 acknowledged that OPAHs were mainly derived from the secondary formation of parent PAH and

238 O_3 and OH radicals (Ambade et al., 2023). It was assumed that both of O_3 and OH radicals were

239 higher in the tropical oceans compared with the temperate and southern oceans based on GEOS-

240 Chem model (Figure S3). The correlation analysis also suggested that the OPAHs concentrations

241 displayed good relationship with O_3 level (r = 0.55, p < 0.05). In addition, the ratios of OPAH/PAH

242 in ECS, WP, BS, EAS, and AO were 13, 7, 53, 26, and 13, respectively. We could find that the

243 oxidation capacities of PAH in BS and EAS were much higher compared with other oceans, though

244 the primary emission of PAH in BS was relatively low. All of these results demonstrated that the

245 strong oxidation capacity of O_3 and OH radical promoted the higher OPAHs concentrations. Most

246 of the OPAH species displayed similar spatial variations with the total OPAHs concentrations, while

247 few components such as 1-Naphthaldehyd, Ancenaphthenaquinone, and 6H-Benzo(cd)pyrene-6-

248 one levels in ECS were still higher than those in EAS. It might be linked with the emission intensity

249 of their precursors.

250   Both of RPAHs and NPAHs showed the higher levels in ECS (20 and 3.6 pg/m^3) and WP

251 (22 ± 13 and 3.0 ± 1.2 pg/m^3), which were significantly higher than those in other seas. Among all of

252 the species of RPAHs and NPAHs, 1-Methylnaphthalene and 2-Nitronaphthalene exhibited

253 significantly higher concentrations in ECS (1.61 and 3.61 pg/m^3) and WP (2.1 ± 1.3 and 2.8 ± 1.1

254 pg/m^3) compared with other regions (Figure S4 and S5) ($p < 0.05$). It has been well documented

255 that both of these species were derived from diesel vehicle emission. Southeast Asia and East Asia

256 showed the higher diesel vehicle emission of parent PAHs compared with Australia and some

257 countries in the Southern hemisphere (Shen et al., 2013).

258   Besides, some key meteorological factors including 2-m air temperature (T), 2-m dewpoint

259 temperature (Dew), precipitation (Prec), and wind speed (WS) were also selected to assess their

260   impacts on PAH derivatives (Figure 4). The result suggested that most of PAH derivatives showed

261   significant negative correlation with nearly all of the meteorological parameters. Among all of the

262   meteorological parameters, WS showed the highest correlation coefficients with all of the PAH

263   derivatives, indicating that dilution and diffusion conditions significantly affected their fate because

264   most of these compounds showed relatively long lifetime. Besides, T also showed the higher

265   negative correlation with PAH derivatives because the gas-particle partitioning of PAHs was mainly

266   controlled by the air temperature (Li et al., 2020; Wang et al., 2019b). High air temperature usually

267   suppresses gaseous to particulate sorption of PAH derivatives to marine aerosol, and compound-

268   dependent adsorption kinetics in the atmosphere (Andreae, 1983; Gustafson and Dickhut, 1996;

269   Wang et al., 2019a). Although rainfall washout might be an important pathway for PAH decrease,

270   the correlation coefficients of Prec and PAH derivatives were slightly lower than other

271   meteorological factors. It was assumed that the sampling period showed less rainfall events, and

272   thus the PAH derivatives were not sensitive to Prec..

273   3.3 Source apportionment of parent PAH and derivatives

274   The diagnostic ratio between PAHs has been widely utilized to identify the major sources of

275   particulate PAHs. Based on previous studies, the Fluoran/(Fluoran +Pyr) ratio could be applied to

276   distinguish the potential sources. The ratios less than 0.4, 0.4-0.5, and greater than 0.5 could be

277   treated to be petrogenic source (0.4), petroleum combustion or biomass burning (0.4-0.5), and the

278   coal combustion (> 0.5), respectively (Yunker et al., 2002; Zhang et al., 2021a). In our study, the

279   Fluoran/(Fluoran +Pyr) ratio in nearly all of the regions except AO (0.46) were higher than 0.5,

280   indicating the impact of coal combustion on marine aerosols in most regions in Northern

281   Hemisphere and tropical regions. The geochemical index method shows some uncertainties, and

282   thus it is necessary to employ more diagnostic ratios to enhance the reliability. BaP/BghiP ratio was

283   also widely applied to separate the sources of vehicle emission (≤ 0.6) and coal burning (> 0.6).

284   Both of BS (0.90) and EAS (0.84) showed the higher BaP/BghiP ratios, indicating the important

285   impact of coal combustion on the local marine aerosol (Katsoyiannis et al., 2007). However, the

286   ratio in ECS was much lower than 0.6, indicating that the vehicle or shipping emission also plays a

287   significant role on the local aerosol. Meanwhile, the BaP/(BaP+CT) ratios in ECS and WP reached

288   0.09 and 0.31, respectively. The result fills in the domain derived from diesel emission, which

further supported the inference that the marine aerosols in both of ECS and WP were significantly affected by diesel emission (Ma et al., 2020). For AO, all of the diagnostic ratios suggested that the oceans were mainly affected by shipping emission and wood burning.

Although the geochemical index method could identify the potential sources of PAH species, the contributions of multiple sources to PAHs and their derivatives still remained unknown. Therefore, positive matrix factorization (version PMF 5.0) was utilized to determine more source information of PAH species. After 30 runs, the optimal three factors with the lowest values of Q (robust) and Q (true) were determined. Factor 1 (56%) possesses the higher loadings of Fluoran, BaA, CT, BeP, BaP, and 1-Methylnaphthalene (Figure 5). It was well known that Fluoran and BaA were typical indicators for coal combustion (Wang et al., 2016). Meanwhile, BeP, BaP, and 1-Methylnaphthalene were often derived from shipping emission (Li et al., 2022). Therefore, factor 1 could be defined as the mixed source of coal burning and engine combustion emission. Factor 2 (30%) shows a high correlation with LMW PAHs such as Nap, Flu, Phe, Ant, BbF. It was well documented that these LMW PAH species mainly originated from wood and biomass burning (Chen et al., 2022; Zhang et al., 2021a; Zhang et al., 2020). Factor 3 (14%) is characterized by medium and high contributions of 5,12-Naphthacenequione, 1,6,7-Trimethylnaphthalene, and 2-Nitronaphthalene. Many previous studies have confirmed that the photochemical reaction involving NO_2 initiated by OH radicals was highly effective for the production of 2-Nitronaphthalene in $PM_{2.5}$ (Arey et al., 1990; Atkinson et al., 1990). Hence, the factor could be treated to be the secondary formation. Based on the source apportionment, we verified that EAS showed relatively high secondary contribution compared with some regions such ECS and WP. It was assumed that EAS showed the higher atmospheric oxidates and low PAH emissions (Ambade et al., 2023; Shen et al., 2013), which was in good agreement the spatial variations of PAHs and OPAHs.

4   Conclusions and implications

In summary, our study verifies the ubiquitous occurrence of PAHs and their derivatives in the aerosols of the Western Pacific (WP), Bismarck Sea (BS), East Australian Sea (EAS), and even the Antarctica Ocean (AO). The highest PAH concentrations in marine aerosols were observed in WP (447±228 pg/m³), followed by the East China Sea (ECS) (195 pg/m³), AO (111±91 pg/m³), EAS (104±88 pg/m³), and the lowest in BS (17±12 pg/m³). PAH derivatives (e.g., OPAHs, RPAHs, and

NPAHs) also showed higher concentrations in WP. The spatial characteristics of these components can be related to precursor emissions and oxidation patterns (e.g., OH/NO_3 radicals, O_3).

For instance, the higher PAH and derivative concentrations observed in WP were primarily due to higher anthropogenic emissions from coal and engine combustion. PAH concentrations in AO were even higher than those in EAS and BS, while OPAH levels in EAS were much higher than those in AO. It is widely acknowledged that OPAHs mainly originate from the secondary formation of parent PAHs through reactions with O_3 and OH radicals. The concentrations of O_3 and OH radicals are higher in tropical oceans compared to temperate and southern oceans.

Both of geochemical index methods and the PMF model suggested that PAHs and their derivatives in global marine aerosols are controlled by three major sources: coal burning and engine combustion emissions (56%), wood and biomass burning (30%), and secondary formation (14%). Marine aerosols in ECS and WP were dominated by coal burning and engine combustion, while BS and EAS were mainly influenced by wildfires and coal combustion. AO was significantly affected by biomass burning and local shipping emissions.

However, this study has some limitations. Firstly, it focuses only on particle-phase PAHs and derivatives, while gas-phase PAH species were not measured. Additionally, data on PAHs in seawater were lacking. Future research should investigate gas-particle partitioning and the exchange processes between air and seawater phases in the global marine environment. Moreover, our study did not include cruise observations of marine aerosols in the Atlantic and Arctic Oceans. Future studies should collect marine aerosols from all major oceans. Furthermore, measuring the concentrations of PAHs and derivatives in marine aerosols over multiple years will help analyze the impact of changes in anthropogenic emissions on these components, providing insight into their spatial distribution and fate (formation or removal mechanisms).

Acknowledgements

This work was supported by the National Natural Science Foundation of China (42107113, 42276243), and the Fundamental Research Funds for the Central Universities. The authors are grateful to the CHINARE members for their support and assistance in atmosphere sampling.

Data Availability Statement

The data presented in this study are available at the Zenodo data archive

347   https://zenodo.org/records/14291911 (Li et al., 2024).

348   **Author Contributions**

349   Conceptualization: Rui Li, Xing Liu, and Guitao Shi; Data Curation: Yubing Shen, Yumeng Shao,

350   and Yining Gao; Formal analysis: Ziwei Yao, Qian Liu

351   **Competing interests**

352   The contact author has declared that none of the authors has any competing interests.

353

References

354

355   Ambade, B., Sethi, S.S., Chintalacheruvu, M.R. (2023) Distribution, risk assessment, and

356   source apportionment of polycyclic aromatic hydrocarbons (PAHs) using positive matrix

357   factorization (PMF) in urban soils of East India. Environmental geochemistry and health 45, 491-

358   505.

359   Andreae, M.O. (1983) Soot carbon and excess fine potassium: Long-range transport of

360   combustion-derived aerosols. Science 220, 1148-1151.

361   Arey, J., Atkinson, R., Aschmann, S.M., Schuetzle, D. (1990) Experimental investigation of

362   the atmospheric chemistry of 2-methyl-1-nitronaphthalene and a comparison of predicted nitroarene

363   concentrations with ambient air data. Polycyclic Aromatic Compounds 1, 33-50.

364   Atkinson, R., Arey, J., Zielinska, B., Aschmann, S.M. (1990) Kinetics and nitro-products of

365   the gas-phase OH and NO3 radical-initiated reactions of naphthalene-d8, Fluoranthene-d10, and

366   pyrene. International Journal of Chemical Kinetics 22, 999-1014.

367   Bandowe, B.A.M., Meusel, H. (2017) Nitrated polycyclic aromatic hydrocarbons (nitro-PAHs)

368   in the environment–a review. Science of the Total Environment 581, 237-257.

369   Cabrerizo, A., Galbán-Malagón, C., Del Vento, S., Dachs, J. (2014) Sources and fate of

370   polycyclic aromatic hydrocarbons in the Antarctica and Southern Ocean atmosphere. Global

371   Biogeochemical Cycles 28, 1424-1436.

372   Chen, Y.-P., Zeng, Y., Guan, Y.-F., Huang, Y.-Q., Liu, Z., Xiang, K., Sun, Y.-X., Chen, S.-J.

373   (2022) Particle size-resolved emission characteristics of complex polycyclic aromatic hydrocarbon

374   (PAH) mixtures from various combustion sources. Environmental Research 214, 113840.

375   Gao, B., Wang, X.-M., Zhao, X.-Y., Ding, X., Fu, X.-X., Zhang, Y.-L., He, Q.-F., Zhang, Z.,

376   Liu, T.-Y., Huang, Z.-Z. (2015) Source apportionment of atmospheric PAHs and their toxicity using

377   PMF: Impact of gas/particle partitioning. Atmospheric Environment 103, 114-120.

378   Gustafson, K.E., Dickhut, R.M. (1996) Particle/gas concentrations and distributions of PAHs

379   in the atmosphere of southern Chesapeake Bay. Environmental science & technology 31, 140-147.

380   Haque, M.K., Azad, M.A.K., Hossain, M.Y., Ahmed, T., Uddin, M., Hossain, M.M. (2021)

381   Wildfire in Australia during 2019-2020, Its impact on health, biodiversity and environment with

382   some proposals for risk management: a review. Journal of Environmental Protection 12, 391-414.

383   Jaeckels, J.M., Bae, M.-S., Schauer, J.J. (2007) Positive matrix factorization (PMF) analysis of

384 molecular marker measurements to quantify the sources of organic aerosols. Environmental science

385 & technology 41, 5763-5769.

386   Kang, M., Yang, F., Ren, H., Zhao, W., Zhao, Y., Li, L., Yan, Y., Zhang, Y., Lai, S., Zhang, Y.

387 (2017) Influence of continental organic aerosols to the marine atmosphere over the East China Sea:

388 Insights from lipids, PAHs and phthalates. Science of the Total Environment 607, 339-350.

389   Katsoyiannis, A., Terzi, E., Cai, Q.-Y. (2007) On the use of PAH molecular diagnostic ratios in

390 sewage sludge for the understanding of the PAH sources. Is this use appropriate? Chemosphere 69,

391 1337-1339.

392   Kovacic, P., Somanathan, R. (2014) Nitroaromatic compounds: Environmental toxicity,

393 carcinogenicity, mutagenicity, therapy and mechanism. Journal of Applied Toxicology 34, 810-824.

394   Li, B., Zhou, S., Wang, T., Zhou, Y., Ge, L., Liao, H. (2020) Spatio-temporal distribution and

395 influencing factors of atmospheric polycyclic aromatic hydrocarbons in the Yangtze River Delta.

396 Journal of Cleaner Production 267, 122049.

397   Li, C., Li, Z., Wang, H. (2023) Characterization and risk assessment of polycyclic aromatic

398 hydrocarbons (PAHs) pollution in particulate matter in rural residential environments in China-A

399 review. Sustainable Cities and Society, 104690.

400   Li, D., Zhao, Y., Du, W., Zhang, Y., Chen, Y., Lei, Y., Wu, C., Wang, G. (2022) Characterization

401 of PM2. 5-bound parent and oxygenated PAHs in three cities under the implementation of Clean Air

402 Action in Northern China. Atmospheric Research 267, 105932.

403   Li, R., Hua, P., Krebs, P. (2021a) Global trends and drivers in consumption-and income-based

404 emissions of polycyclic aromatic hydrocarbons. Environmental science & technology 56, 131-144.

405   Li, R., Shen, Y., Shao, Y., Gao, Y., Yao, Z., Liu, Q., Liu, X., Shi, G. (2024) Measurement Report:

406 Polycyclic aromatic hydrocarbons (PAHs) and their alkylated (RPAHs), nitrated (NPAHs) and

407 oxygenated (OPAHs) derivatives in the global marine atmosphere: occurrence, spatial variations,

408 and source apportionment. Atmospheric Chemistry and Physics.

409   Li, Y., Liu, M., Hou, L., Li, X., Yin, G., Sun, P., Yang, J., Wei, X., He, Y., Zheng, D. (2021b)

410 Geographical distribution of polycyclic aromatic hydrocarbons in estuarine sediments over China:

411 Human impacts and source apportionment. Science of the Total Environment 768, 145279.

Lian, L., Huang, T., Ke, X., Ling, Z., Jiang, W., Wang, Z., Song, S., Li, J., Zhao, Y., Gao, H. (2021) Globalization-driven industry relocation significantly reduces arctic PAH contamination. Environmental science & technology 56, 145-154.

Ma, L., Li, B., Liu, Y., Sun, X., Fu, D., Sun, S., Thapa, S., Geng, J., Qi, H., Zhang, A. (2020) Characterization, sources and risk assessment of PM2. 5-bound polycyclic aromatic hydrocarbons (PAHs) and nitrated PAHs (NPAHs) in Harbin, a cold city in Northern China. Journal of Cleaner Production 264, 121673.

Neroda, A.S., Goncharova, A.A., Mishukov, V.F. (2020) PAHs in the atmospheric aerosols and seawater in the North–West Pacific Ocean and Sea of Japan. Atmospheric Environment 222, 117117.

Pegoraro, C.N., Quiroga, S.L., Montejano, H.A., Rimondino, G.N., Argüello, G.A., Chiappero, M.S. (2020) Assessing polycyclic aromatic hydrocarbons in the marine atmosphere on a transect across the Southwest Atlantic Ocean. Atmospheric Pollution Research 11, 1035-1041.

Pietrogrande, M.C., Abbaszade, G., Schnelle-Kreis, J., Bacco, D., Mercuriali, M., Zimmermann, R. (2011) Seasonal variation and source estimation of organic compounds in urban aerosol of Augsburg, Germany. Environmental pollution 159, 1861-1868.

Sevimoglu, O., Rogge, W.F. (2016) Seasonal size-segregated PM10 and PAH concentrations in a rural area of sugarcane agriculture versus a coastal urban area in Southeastern Florida, USA. Particuology 28, 52-59.

Sharma, S., Mandal, T., Jain, S., Saraswati, Sharma, A., Saxena, M. (2016) Source apportionment of $PM_{2.5}$ in Delhi, India using PMF model. Bulletin of environmental contamination and toxicology 97, 286-293.

Shen, H., Huang, Y., Wang, R., Zhu, D., Li, W., Shen, G., Wang, B., Zhang, Y., Chen, Y., Lu, Y. (2013) Global atmospheric emissions of polycyclic aromatic hydrocarbons from 1960 to 2008 and future predictions. Environmental science & technology 47, 6415-6424.

Taghvaee, S., Sowlat, M.H., Mousavi, A., Hassanvand, M.S., Yunesian, M., Naddafi, K., Sioutas, C. (2018) Source apportionment of ambient PM2. 5 in two locations in central Tehran using the Positive Matrix Factorization (PMF) model. Science of the Total Environment 628, 672-686.

Van Overmeiren, P., Demeestere, K., De Wispelaere, P., Gili, S., Mangold, A., De Causmaecker, K., Mattielli, N., Delcloo, A., Langenhove, H.V., Walgraeve, C. (2024) Four Years of Active

Sampling and Measurement of Atmospheric Polycyclic Aromatic Hydrocarbons and Oxygenated Polycyclic Aromatic Hydrocarbons in Dronning Maud Land, East Antarctica. Environmental science & technology 58, 1577-1588.

Wang, J., Ho, S.S.H., Huang, R., Gao, M., Liu, S., Zhao, S., Cao, J., Wang, G., Shen, Z., Han, Y. (2016) Characterization of parent and oxygenated-polycyclic aromatic hydrocarbons (PAHs) in Xi'an, China during heating period: An investigation of spatial distribution and transformation. Chemosphere 159, 367-377.

Wang, L., Dong, S., Liu, M., Tao, W., Xiao, B., Zhang, S., Zhang, P., Li, X. (2019a) Polycyclic aromatic hydrocarbons in atmospheric PM2. 5 and PM10 in the semi-arid city of Xi'an, Northwest China: Seasonal variations, sources, health risks, and relationships with meteorological factors. Atmospheric Research 229, 60-73.

Wang, Y., Zhang, Q., Zhang, Y., Zhao, H., Tan, F., Wu, X., Chen, J. (2019b) Source apportionment of polycyclic aromatic hydrocarbons (PAHs) in the air of Dalian, China: Correlations with six criteria air pollutants and meteorological conditions. Chemosphere 216, 516-523.

Wei, C., Bandowe, B.A.M., Han, Y., Cao, J., Watson, J.G., Chow, J.C., Wilcke, W. (2021) Polycyclic aromatic compounds (PAHs, oxygenated PAHs, nitrated PAHs, and azaarenes) in air from four climate zones of China: Occurrence, gas/particle partitioning, and health risks. Science of the Total Environment 786, 147234.

Wietzoreck, M., Kyprianou, M., Musa Bandowe, B.A., Celik, S., Crowley, J.N., Drewnick, F., Eger, P., Friedrich, N., Iakovides, M., Kukučka, P. (2022) Polycyclic aromatic hydrocarbons (PAHs) and their alkylated, nitrated and oxygenated derivatives in the atmosphere over the Mediterranean and Middle East seas. Atmospheric Chemistry and Physics 22, 8739-8766.

Yan, Y., He, Q., Guo, L., Li, H., Zhang, H., Shao, M., Wang, Y. (2017) Source apportionment and toxicity of atmospheric polycyclic aromatic hydrocarbons by PMF: Quantifying the influence of coal usage in Taiyuan, China. Atmospheric Research 193, 50-59.

Yunker, M.B., Macdonald, R.W., Vingarzan, R., Mitchell, R.H., Goyette, D., Sylvestre, S. (2002) PAHs in the Fraser River basin: a critical appraisal of PAH ratios as indicators of PAH source and composition. Organic geochemistry 33, 489-515.

Zetterdahl, M., Moldanova, J., Pei, X.Y., Pathak R.V., Demirdjian, B. (2016) Impact of the 0.1%

fuel sulfur content limit in SECA on particle and gaseous emissions from marine vessels. Atmospheric Environment 145, 338-345.

Zhang, L., Yang, L., Bi, J., Liu, Y., Toriba, A., Hayakawa, K., Nagao, S., Tang, N. (2021a) Characteristics and unique sources of polycyclic aromatic hydrocarbons and nitro-polycyclic aromatic hydrocarbons in PM$_{2.5}$ at a highland background site in northwestern China ☆ . Environmental pollution 274, 116527.

Zhang, L., Yang, L., Zhou, Q., Zhang, X., Xing, W., Wei, Y., Hu, M., Zhao, L., Toriba, A., Hayakawa, K. (2020) Size distribution of particulate polycyclic aromatic hydrocarbons in fresh combustion smoke and ambient air: A review. Journal of Environmental Sciences 88, 370-384.

Zhang, P., Zhou, Y., Chen, Y., Yu, M., Xia, Z. (2023) Construction of an atmospheric PAH emission inventory and health risk assessment in Jiangsu, China. Air Quality, Atmosphere & Health 16, 629-640.

Zhang, R., Han, M., Yu, K., Kang, Y., Wang, Y., Huang, X., Li, J., Yang, Y. (2021b) Distribution, fate and sources of polycyclic aromatic hydrocarbons (PAHs) in atmosphere and surface water of multiple coral reef regions from the South China Sea: A case study in spring-summer. Journal of hazardous materials 412, 125214.

Zhang, X., Zhang, Z.-F., Zhang, X., Zhu, F.-J., Li, Y.-F., Cai, M., Kallenborn, R. (2022a) Polycyclic aromatic hydrocarbons in the marine atmosphere from the Western Pacific to the Southern Ocean: Spatial variability, Gas/particle partitioning, and source apportionment. Environmental science & technology 56, 6253-6261.

Zhang, Y., Shen, Z., Sun, J., Zhang, L., Zhang, B., Zou, H., Zhang, T., Ho, S.S.H., Chang, X., Xu, H. (2021c) Parent, alkylated, oxygenated and nitrated polycyclic aromatic hydrocarbons in PM2. 5 emitted from residential biomass burning and coal combustion: A novel database of 14 heating scenarios. Environmental pollution 268, 115881.

Zhang, Y., Tao, S. (2009) Global atmospheric emission inventory of polycyclic aromatic hydrocarbons (PAHs) for 2004. Atmospheric Environment 43, 812-819.

Zhang, Z.-F., Chen, J.-C., Zhao, Y.-X., Wang, L., Teng, Y.-Q., Cai, M.-H., Zhao, Y.-H., Nikolaev, A., Li, Y.-F. (2022b) Determination of 123 polycyclic aromatic hydrocarbons and their derivatives in atmospheric samples. Chemosphere 296, 134025.

499   Zimmermann, K., Jariyasopit, N., Massey Simonich, S.L., Tao, S., Atkinson, R., Arey, J. (2013)

500   Formation of nitro-PAHs from the heterogeneous reaction of ambient particle-bound PAHs with

501   N2O5/NO3/NO2. Environmental science & technology 47, 8434-8442.
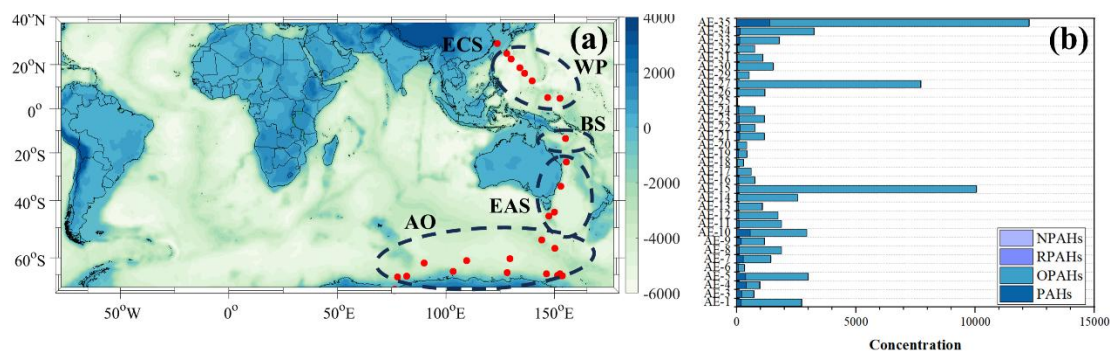
Figure 1 The sampling sites during the cruise from Shanghai to Antarctica (red dots) (a). The total concentrations (Unit: pg/m^3) of PAHs, OPAHs, RPAHs, and NPAHs for all of the samples (from AE-1 to AE-35) (b). The indicators from AE-1 to AE-35 represent the collected aerosol samples in the global marine. ECS, WP, BS, EAS, and AO represent East China Sea, Western Pacific, Bismarck Sea, Eastern Australia Sea, and Antarctic Ocean, respectively.
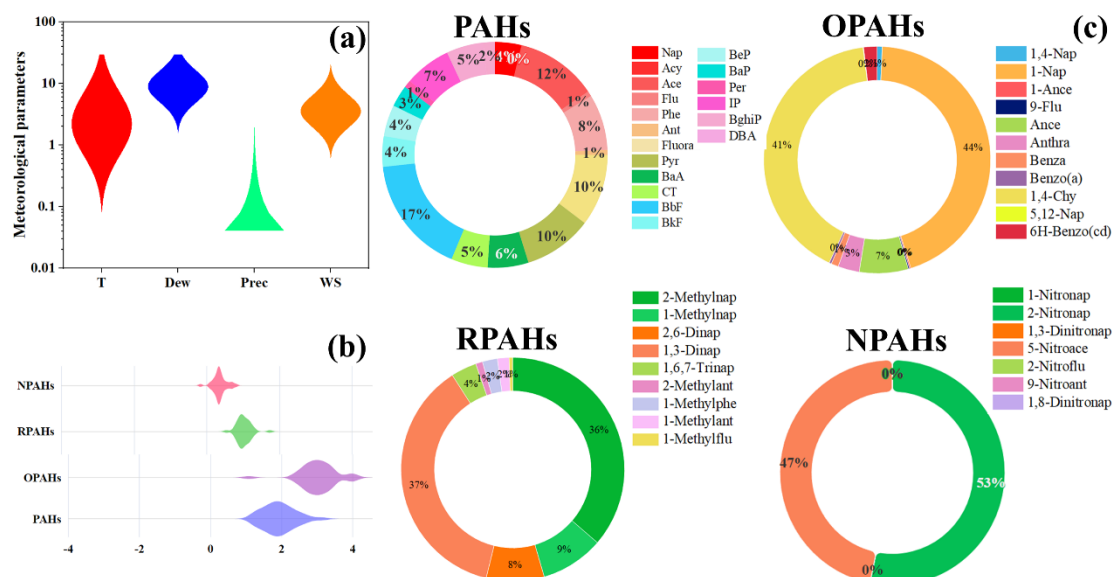
Figure 2 The average meteorological parameters during the cruise (a). T, Dew, Prec, and WS denote 2-m air temperature (Unit: ℃), dewpoint temperature (Unit: ℃), precipitation (mm), and wind speed (m/s), respectively. The average concentrations (log$_{10}$ (concentration), Unit: pg/m^3) of PAHs, OPAHs, RPAHs, and NPAHs for all of the samples (b). The contribution ratios of species in PAHs, OPAHs, RPAHs, and NPAHs (Unit: %) (c). For OPAHs, 1,4-Nap, 1-Nap, 1-Ance, 9-Flu, Ance, Anthra, Benza, Benzo (a), 1,4-Chy, 5,12-Nap, and 6H-Benzo(cd) represent 1,4-Naphthoquinone, 1-Naphthaldehyd, 1-Ancenaphthenaquinone, 9-Fluorenone, Ancenaphthenaquinone, Anthraquinone, Benzanthrone, Benzo(a)anthracene-7,12-dione, 1,4-Chysenequione, 5,12-Naphthacenequione, and 6H-Benzo(cd)pyrene-6-one, respectively. For RPAHs, 2-Methylnap, 1-Methylnap, 2,6-Dinap, 1,3-Dinap, 1,6,7-Trinap, 2-Methylant, 1-Methylphe, 1-Methylant, and 1-Methylflu denote 2-Methylnaphthalene, 1-Methylnaphthalene, 2,6-Dimethylnaphthalene, 1,3-Dimethylnaphthalene, 1,6,7-Trimethylnaphthalene, 2-Methylanthracene, 1-Methylphenanthrene, 1-Methylanthracene, 1-Methylfluoranthene, respectively. For NPAHs, 1-Nitronap, 2-Nitronap, 1,3-Dinitronap, 5-Nitroace, 2-Nitroflu, 9-Nitroant, and 1,8-Dinitronap reflects 1-Nitronaphthalene, 2-Nitronaphthalene, 1,3-Dinitronaphthalene, 5-Nitroacenaphthene, 2-Nitrofluorene, 9-Nitroanthracene, 1,8-Dinitronaphthalene, respectively.

526
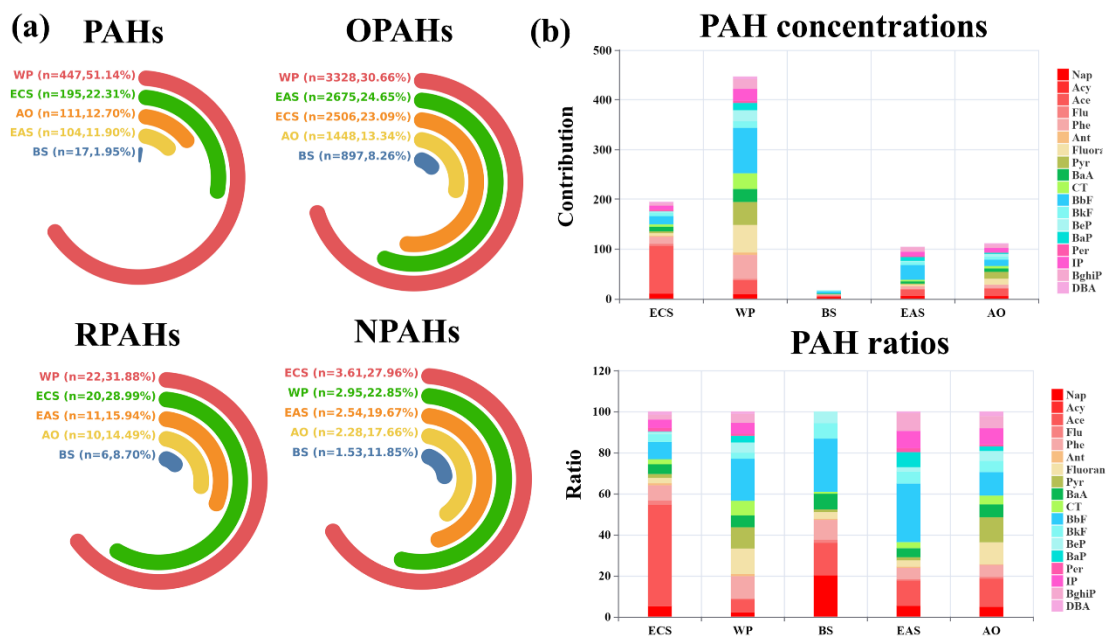
Figure 3 The spatial variations of PAHs and derivatives in the marine aerosols (e.g., n means the average concentration of PAHs and derivatives, and the ratio (%) denotes the quotient of PAHs concentrations in each region and the total concentrations in all of five regions (a). The spatial distributions of PAH species (Unit: pg/m^3) in the global marine aerosols (b).
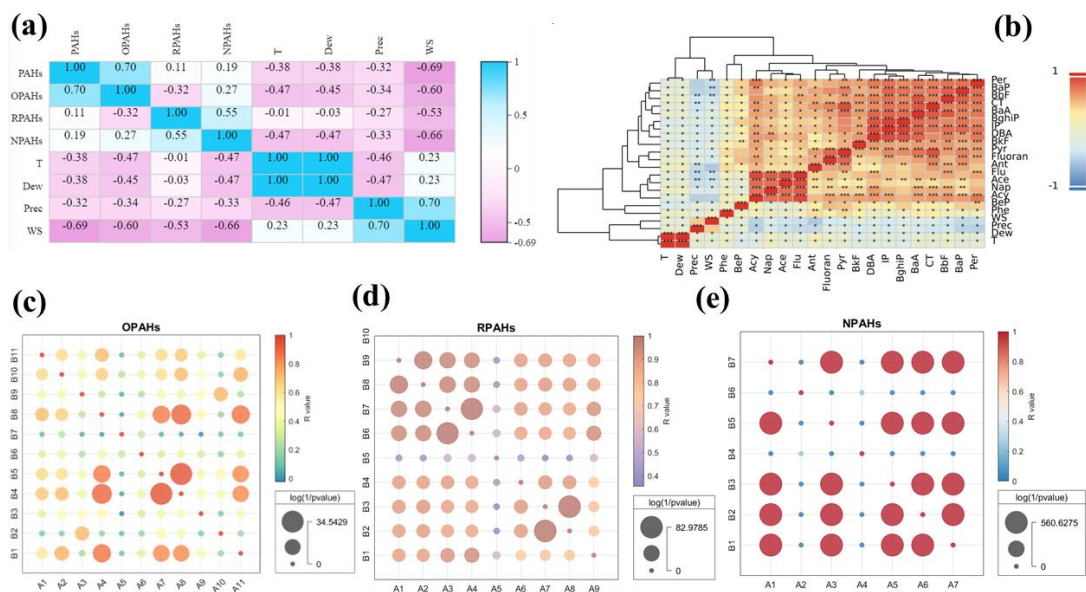
Figure 4 The correlation of PAHs, OPAHs, RPAHs, and NAPHs and meteorological parameters. The correlation of PAH species and meteorological factors (b). The correlation coefficients and log (1/p values) of OPAH species (c). A1 (B1), A2 (B2), A3 (B3), A4 (B4), A5 (B5), A6 (B6), A7 (B7), A8 (B8), A9 (B9), A10 (B10), and A11 (B11) in (c) represent 1,4-Naphthoquinone, 1-Naphthaldehyd, 1-Ancenaphthenaquinone, 9-Fluorenone, Ancenaphthenaquinone, Anthraquinone, Benzanthrone, Benzo(a)anthracene-7,12-dione, 1,4-Chysenequione, 5,12-Naphthacenequione, and 6H-Benzo(cd)pyrene-6-one, respectively. The correlation coefficients and log (1/p values) of RPAH species (d). A1 (B1), A2 (B2), A3 (B3), A4 (B4), A5 (B5), A6 (B6), A7 (B7), A8 (B8), and A9 (B9) in (d) denote 2-Methylnaphthalene, 1-Methylnaphthalene, 2,6-Dimethylnaphthalene, 1,3-Dimethylnaphthalene, 1,6,7-Trimethylnaphthalene, 2-Methylanthracene, 1-Methylphenanthrene, 1-Methylanthracene, 1-Methylfluoranthene, respectively. The correlation coefficients and log (1/p values) of NPAH species (e). A1 (B1), A2 (B2), A3 (B3), A4 (B4), A5 (B5), A6 (B6), and A7 (B7) in (e) reflects 1-Nitronaphthalene, 2-Nitronaphthalene, 1,3-Dinitronaphthalene, 5-Nitroacenaphthene, 2-Nitrofluorene, 9-Nitroanthracene, 1,8-Dinitronaphthalene, respectively.

546
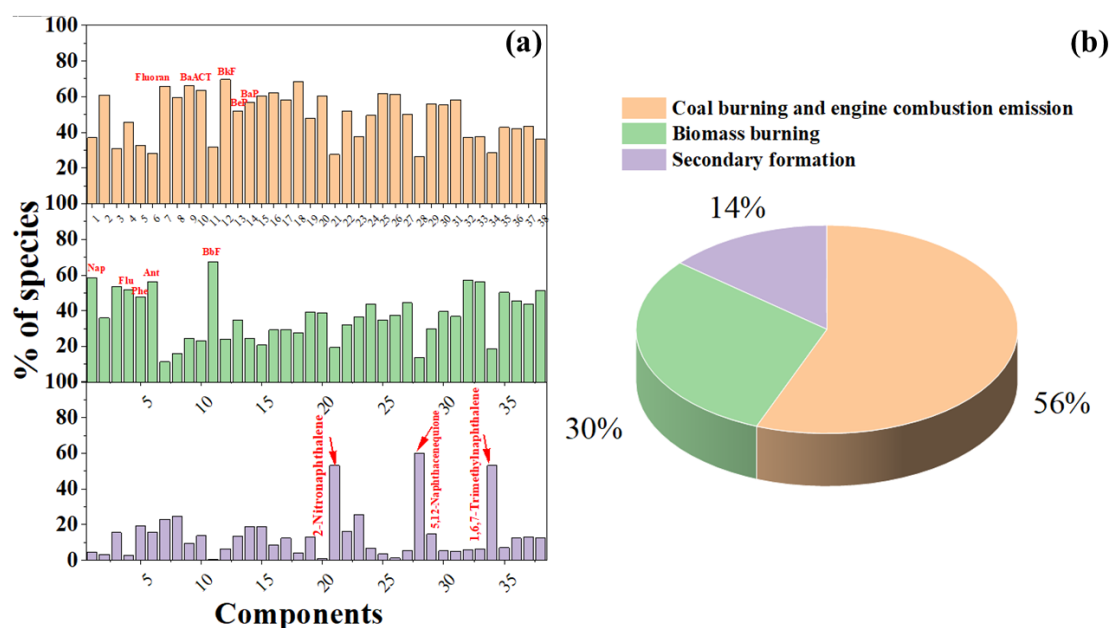
547 **Figure 5** The factor profiles (% of species) resolved from PMF analysis (a). Source contributions

548 of three factors to the total parent PAHs and derivatives in $PM_{2.5}$ at the marine atmosphere (b). The

549 number from 1 to 38 denote Nap, Acy, Ace, Flu, Phe, Ant, Fluoran, Pyr, BaA, CT, BbF, BkF, BeP,

550 BaP, Per, IP, BghiP, DBA, 1,4-Naphthoquinone, 1-Naphthaldehyd, 2-Nitronaphthalene, 1-

551 Ancenaphthenaquinone, 9-Fluorenone, Ancenaphthenaquinone, Anthraquinone, Benzanthrone,

552 Benzo(a)anthracene-7,12-dione, 1,4-Chysenequione, 5,12-Naphthacenequione, 6H-

553 Benzo(cd)pyrene-6-one, 2-Methylnaphthalene, 1-Methylnaphthalene, 2,6-Dimethylnaphthalene,

554 1,3-Dimethylnaphthalene, 1,6,7-Trimethylnaphthalene, 2-Methylanthracene, 1-

555 Methylphenanthrene, and 1-methylanthracene, respectively.